monotherapy for epilepsy in many countries (10), is also a promising candidate for treatment of migraine. Several randomized, double-blind, placebo-controlled multicenter trials have demonstrated that TPM reduces the frequency of migraine and is well tolerated (11–14). It was also shown to improve workplace productivity and quality of life (15,16). The Prolonged Migraine Prevention with TPM (PROMPT) trial revealed that TPM reduced migraine auras in parallel with a reduction of headache, and the effects were similar in patients with and without aura (17). In addition, recent studies in experimental animals, as well as clinical observations, suggest that silent CSD may be involved in migraine without aura (18,19). Thus, there is interest in drugs that suppress CSD as candidates for preventive migraine treatment. The inhibitory effect of TPM on CSD has been investigated in experimental animals (20), including a chronic administration study in rats. In the present work, we examined in detail the effect of 6-week daily oral administration of TPM at various doses on potassium-evoked CSD in anesthetized rats.

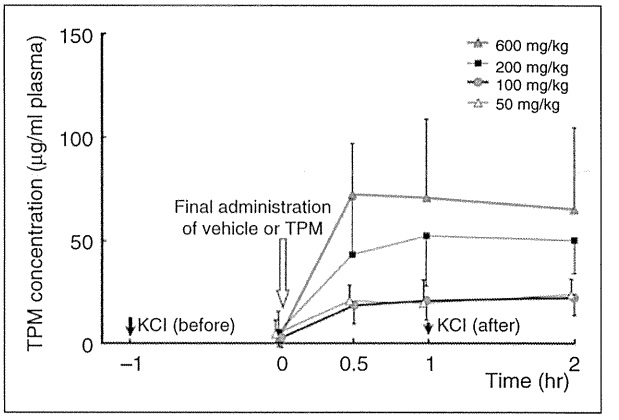

Figure 1. Plasma concentrations of TPM before and after the final administration of TPM on the day of CSD evaluation in chronically treated rats. An outlined arrow indicates the time of final intragastric administration of vehicle/TPM (t = 0) and solid arrows indicate the times of KCl application on the surface of the brain [KCl (before) at t = −1 and KCl (after) at t = 1].

Materials and methods

General procedures of chronic study

Animals were used with the approval (No. 09058) of the Animal Ethics Committee of Keio University (Tokyo, Japan), and all experimental procedures were in accordance with the university's guidelines for the care and use of laboratory animals. Male Sprague-Dawley rats (8–9 weeks, initial body weight; 412 ± 28 g, n = 30) were randomized to five groups so that the mean body weights were not significantly different among groups: a vehicle group (0.5% methylcellulose: 400 cps (centipoises); Sigma Aldrich Japan, Tokyo, Japan) and four TPM groups (50 mg/kg, 100 mg/kg, 200 mg/kg, 600 mg/kg; provided by Janssen Pharmaceutical K.K., Tokyo, Japan). Test solution was adjusted to 5 ml/kg and administered by gavage once daily for 6 weeks. During the administration period, rats received food and water ad libitum. The animals were kept in an air-conditioned room maintained at 23.0 ± 1.0°C and 55 ± 7% humidity with automatic lighting between 08:00 and 20:00. Body weight was monitored daily throughout the treatment period.

Procedures of CSD measurement

On the final treatment day, the animals were anesthetized with isoflurane (2.5–3.0%) and subjected to CSD evaluation as previously reported (21). Briefly, each rat was fixed to a head-holder (SG-3 N modified to be flexible around the horizontal axis, Narishige Scientific Instrument Lab., Tokyo, Japan) and a cranial window of approximately 4 mm in diameter was opened in the left side of the skull at the parieto-temporal region of the cerebral cortex. The dura was removed and the exposed cortex was covered with a cover slip to prevent it from drying out. CSD was induced by introducing a drop (5 μl) of 1.0 M KCl solution into an additional posterior hole of 2 mm in diameter, centered at the coordinates of 7 mm posterior and 2 mm lateral to the bregma. Approximately 1 h after the first KCl application, when no further CSD had occurred for more than 10 min, vehicle or TPM was administered through an intragastric catheter. The second application of KCl was performed 1 h after the final administration of vehicle or TPM, as shown in Figure 1. Arterial blood pressure (ABP) was continuously recorded through a femoral arterial catheter via a surgical strain gage (MLT0670 and ML117, ADInstruments Pty. Ltd., Bella Vista, NSW, Australia). Heart rate (HR) was determined from the ABP wave. Continuous recordings of ABP, HR, cerebral blood flow (CBF) and direct current (DC) potential (see below) were acquired with a multi-channel recorder (PowerLab 8/30, ADInstruments Pty. Ltd.) and recorded with proprietary software (LabChart, ADInstruments Pty. Ltd.) for offline analysis. All procedures were performed at constant body temperature, maintained with a heating-pad and thermocontroller (BWT-100, Bioresearch Center Co., Ltd., Nagoya, Japan). CSD was elicited with KCl solution after confirmation that all parameters had remained stable for at least 10 min.

Table 1. Physiological parameters just before CSD evaluation in chronically treated rats

		Before the last administration		After intragastric administration	
Treatment group	Body weight (g)	MABP (mmHg)	HR (bpm)	MABP (mmHg)	HR (bpm)
Vehicle	545 ± 34	74 ± 10	313 ± 57	83 ± 18	341 ± 50
Topiramate 50 mg/kg	536 ± 41	85 ± 12	349 ± 49	86 ± 10	321 ± 28
Topiramate 100 mg/kg	514 ± 53	75 ± 4	295 ± 17	83 ± 10	285 ± 21
Topiramate 200 mg/kg	509 ± 25	74 ± 10	295 ± 18	76 ± 17	282 ± 25
Topiramate 600 mg/kg	482 ± 24 [a]	84 ± 7	317 ± 36	86 ± 10	300 ± 42

HR, heart rate; MABP, mean arterial blood pressure.
[a] $p<0.05$ significant difference from the vehicle control.

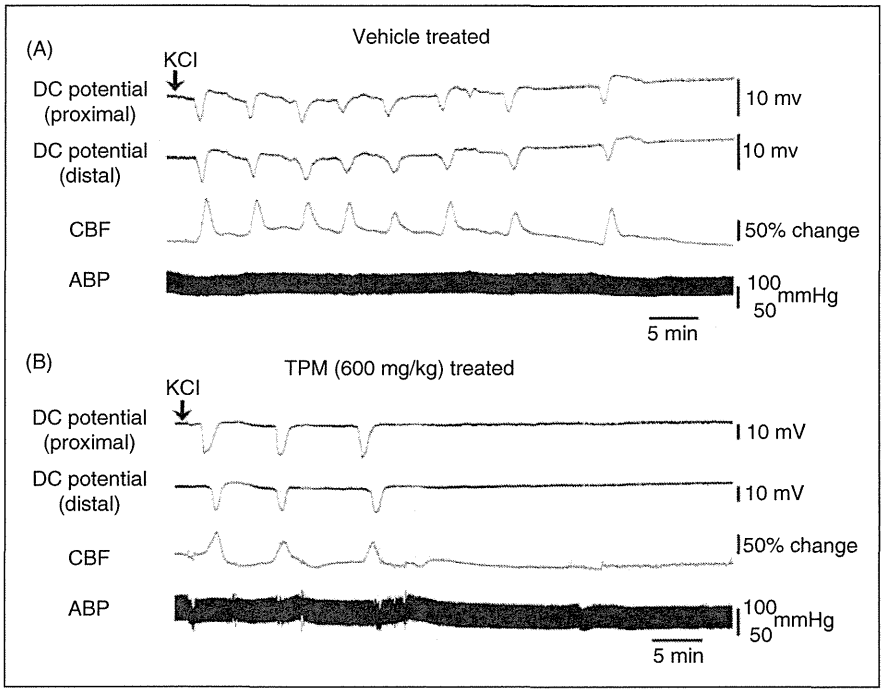

Figure 2. Original recordings of DC potential at the proximal and distal sites, as well as CBF and ABP. KCl was applied on the brain surface at the arrows, 1 h after the final administration of vehicle (A) or 600 mg/kg of TPM (B) in rats treated for 6 weeks.

Measurements of DC potential and CBF

Two Ag/AgCl electrodes (tip diameter = 200 μm, EEG-5002Ag, Bioresearch Center Co., Ltd.) were inserted 200 μm under the pia mater at the anterior edge (0.5 mm posterior and 2 mm lateral to bregma) and posterior edge (3.5 mm posterior and 2 mm lateral to the bregma) of the cranial window, and immobilized with dental cement. Ag/AgCl reference electrodes (EER-5004Ag, Bioresearch Center Co., Ltd.) were subcutaneously placed in the space between the skull-bone and the scalp. DC potential was amplified at 1–100 Hz and digitized at 1 kHz with a differential headstage and differential extracellular amplifier (Model 4002 and EX1, Dagan Co., Minneapolis, MN, USA).

CBF was monitored with a laser Doppler flowmeter (LDF) (ALF 21 R, Advance Co., Ltd., Tokyo, Japan). The probe, which had a diameter of 0.8 mm, was placed on the surface of the cortex 2 mm posterior and 2 mm lateral to the bregma (intermediate region of the cranial window).

Evaluation of CSD susceptibility

One application of KCl induced repetitive negative deflections of DC potential (i.e., CSD). CSD was detected at the posterior site (proximal) and then at the anterior site (distal) after a delay. At the same time, CBF was elevated, as reported previously (21). We defined CSD as the occurrence of DC potential

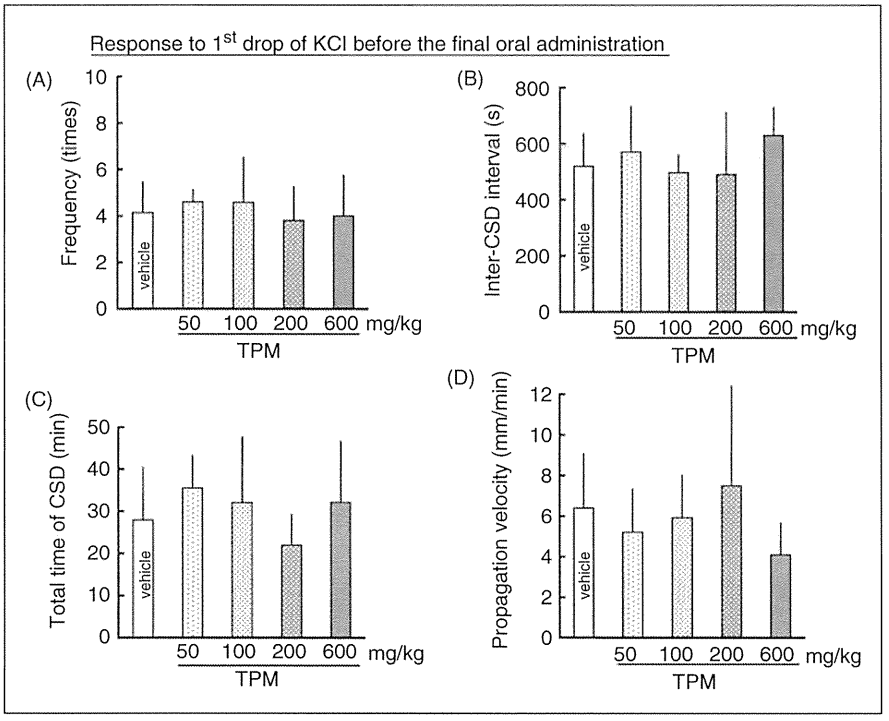

Figure 3. Average values of CSD occurrence frequency (A), inter-CSD interval (B), total length of time for which CSD continued (C) and CSD propagation velocity (D) in response to KCl application 1 h before the final oral administration of vehicle/TPM in chronically treated rats (t = −1 in Figure 1). The results in TPM-treated groups are not statistically significantly different from the vehicle control.

deflections detected at both sites, together with CBF elevation. We evaluated CSD occurrence frequency, interval between CSD episodes, and total length of time for which CSD continued (duration from the first CSD to the last CSD). Propagation velocity from the proximal to the distal site was also calculated based on the distance between the electrodes.

Measurement of plasma level of TPM

Before the final administration of TPM (time 0), and at 30 min, 60 min, and 120 min after the final intragastric administration of TPM, as shown in Figure 1, arterial blood was collected through the arterial catheter. After protein precipitation with acetonitrile, plasma samples were used for measurement of the plasma level of TPM by means of a validated liquid chromatography–tandem mass spectrometry (LC-MS/MS) method (22) with some modifications. Separation was done on a reversed-phase LC column (X-Bridge C18 3.5 μm – 50 × 4.6 mm, Waters, Milford, USA) with a mixture of 10 mM ammonium acetate and acetonitrile as the mobile phase. Detection was by tandem MS on an API-3000 MS/MS (Applied Biosystems, Toronto, Canada), operated in the negative ion mode using the TurboIonSpray^{TM}-interface. TPM was monitored at the m/z transition 338.1 → 78.0 using a dwell time of 300 ms. The limit of quantification was 50 ng/ml. In measurement of independent QC samples, the intra-batch accuracy was between 85% and 115%.

Acute effect of TPM on CSD

Male Sprague-Dawley rats (12–19 weeks, body weight; 519 ± 95 g, n = 7) were used for evaluation of the effect of single administration of TPM. Using the same protocol as described for chronically treated rats, we evaluated the KCl-induced CSD profile and CBF before and after intragastric administration of TPM (600 mg/kg). Changes of ABP, HR and blood gas level were followed. Arterial blood gas analysis was performed with a RapidLab 348 (Siemens AG, Munich, Germany).

Statistical analysis

All data are reported as means ± SD. Multiple comparisons were performed using Dunnett's test among vehicle and TPM chronic administration groups. The paired t-test was used to evaluate the acute effect of TPM on the CSD profile versus the pre-administration

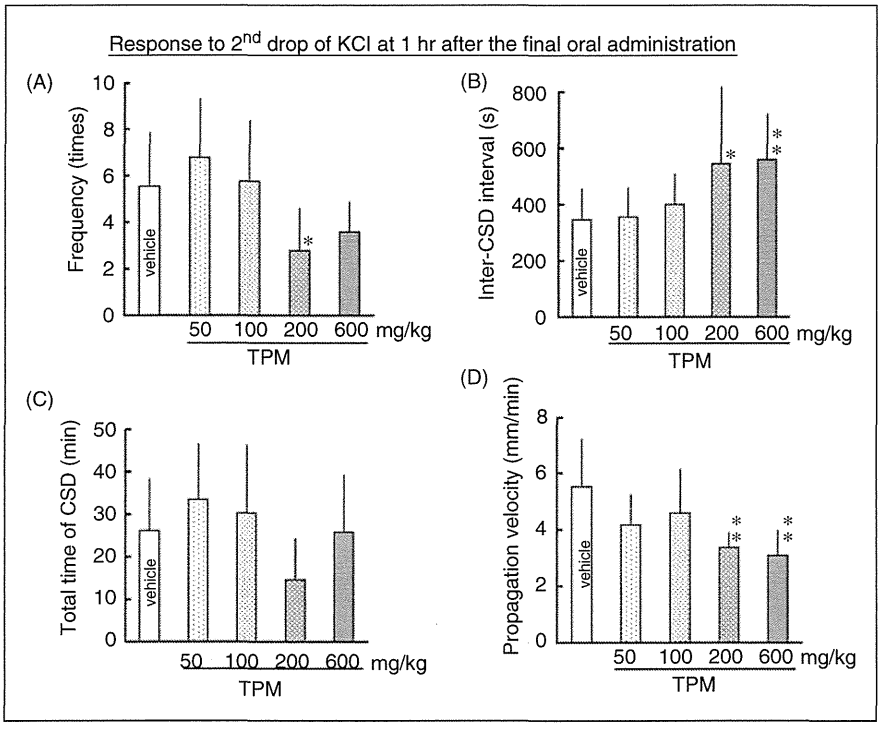

Figure 4. Average values of CSD occurrence frequency (A), inter-CSD interval (B), total length of time for which CSD continued (C) and CSD propagation velocity (D) in response to KCl application 1 h after the final oral administration of vehicle/TPM in chronically treated rats (t = 1 in Figure 1). *p < 0.05, **p < 0.01 significant differences of the TPM-treated groups from the vehicle control.

level. A p value of <0.05 versus the vehicle treatment group or the pre-administration level was considered to be statistically significant.

Results

Plasma level of TPM

The plasma level of TPM increased rapidly after administration, and a dose-dependent plateau level was maintained for 2 h (Figure 1). After 6 weeks of daily administration, the plasma level of TPM before the final administration was 1/5 to 1/50 of the maximum level; that is, there was no indication of TPM accumulation. After intraperitoneal administration of 200 or 500 mg/kg TPM, the plasma level reached a maximum of 125 ± 14 or 155 ± 98 μg/ml, respectively, within 1 h after administration. The maximum plasma level after intragastric administration was approximately 1/3 of that after intraperitoneal administration and remained at a plateau level for a longer period.

Effect of chronic TPM on CSD

Physiological parameters just before CSD evaluation in each group are shown in Table 1. Although dose-dependent suppression of growth was observed, physiological parameters were not significantly different among the treated group. Neither mortality nor abnormal behavior was observed in any animal during the treatment period. Therefore, we concluded that the physiological state of the animals was not impaired.

As shown in Figure 2A, one application of KCl induced repetitive (between 2 and 8 times) negative deflections of DC potential (i.e., CSD). CSD was detected first at the posterior (proximal) site, and then at the anterior (distal) site with a delay time of 14 to 80 s. After the final administration of TPM, CSD occurrence was slightly suppressed (Figure 2B). No CSD-associated change of ABP was seen in any rat. Mean arterial blood pressure (MABP) was maintained within ± 20 mmHg in each rat throughout the experiments, and did not decrease below 60 mmHg in any rat.

In the observation 1 h before the final oral administration of TPM, none of CSD occurrence frequency, inter-CSD interval, total length of time for which CSD continued or propagation velocity was statistically significantly different from the value in the vehicle group (Figure 3). However, 1 h after the final oral administration of TPM, during the plasma TPM level plateau period, CSD occurrence frequency was dose-dependently decreased, inter-CSD interval was

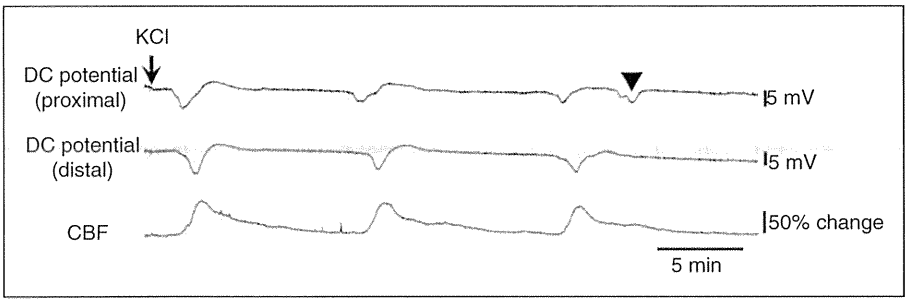

Figure 5. Original recordings of DC potential at the proximal and distal sites and CBF showing an example of non-propagated DC potential deflection. DC potential deflection detected at the proximal site was not propagated to the distal site, as indicated with an arrowhead, and there was no CBF change.

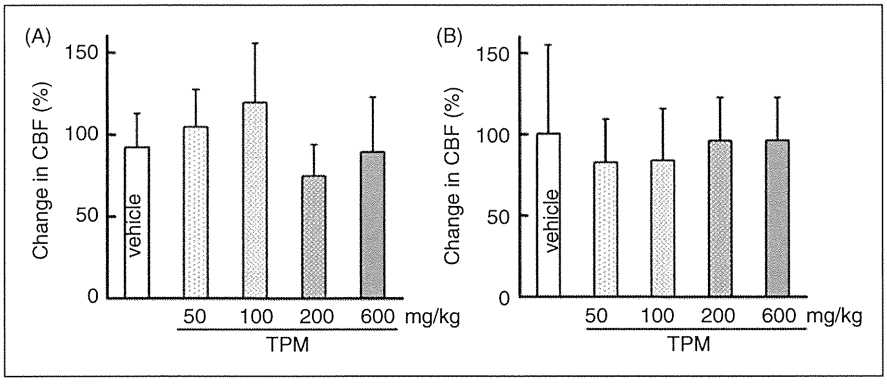

Figure 6. Average values of CSD-associated CBF changes in response to KCl application before the final oral administration of drugs ($t = -1$ in Figure 1) (A) and those in response to KCl application after the final oral administration of drugs ($t = 1$ in Figure 1) (B). There are no statistically significant differences from the vehicle control.

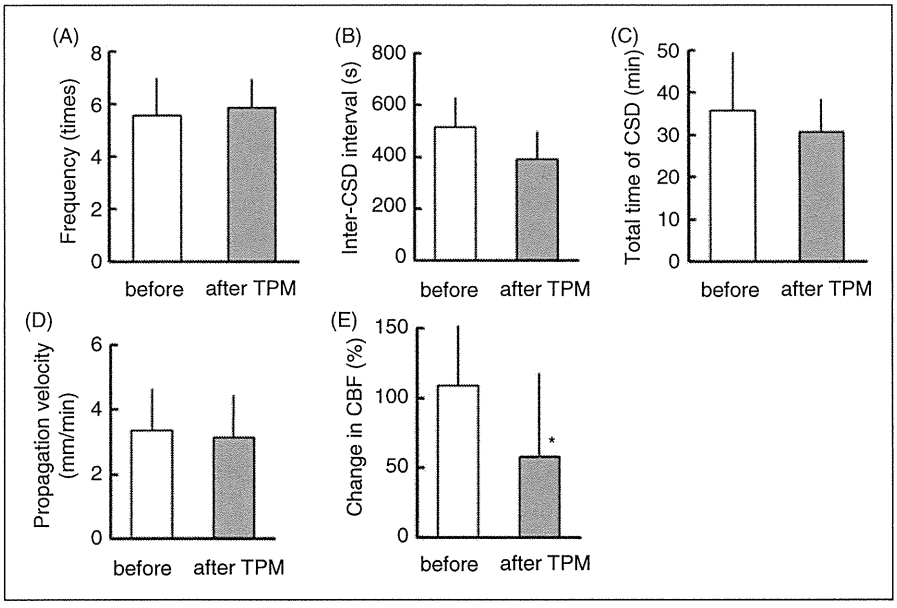

Figure 7. Changes of CSD occurrence frequency (A), inter-CSD interval (B), total length of time for which CSD continued (C), CSD propagation velocity (D) and CSD-associated CBF changes (E) from the pre-administration level (before) to the level after single gavage administration of TPM (600 mg/kg). *$p < 0.05$ significant difference from the pre-administration level.

Table 2. Changes in physiological parameters, arterial pH and arterial blood gas in response to CSD induction with KCl application

	MABP (mmHg)	HR (bpm)	pH	PaO_2 (mmHg)	$PaCO_2$ (mmHg)
Before administration of topiramate					
Before KCl	80 ± 5	320 ± 22	7.46 ± 0.01	84 ± 8	39 ± 3
After 1 h	80 ± 6	308 ± 24	7.45 ± 0.03	78 ± 10	38 ± 3
After intragastric administration of topiramate					
Before KCl	82 ± 14	298 ± 36	7.42 ± 0.04	88 ± 9	38 ± 4
After 1 h	76 ± 13	288 ± 32	7.41 ± 0.04	81 ± 6	40 ± 4

HR, heart rate; MABP, mean arterial blood pressure; PaO_2, partial pressure of arterial oxygen; $PaCO_2$, partial pressure of arterial carbon dioxide.

elongated, and propagation velocity was decreased. The total length of time for which CSD continued showed a tendency to decrease, but this was not significant (Figure 4). A small negative deflection of DC potential only at the proximal site but not at the distal site, with a small CBF change or with no CBF change, was detected in seven rats (three rats in the 600 mg/kg group, two rats in the 100 mg/kg group, one rat in the 50 mg/kg group and one rat in the vehicle group) (Figure 5). There was no difference in the CSD-associated elevation of CBF before and after the final administration of TPM (Figure 6).

Acute effect of TPM on CSD

KCl-induced CSD susceptibility (CSD occurrence frequency, inter-CSD interval, propagation velocity and total length of time for which CSD continued) was not significantly influenced, but CSD-associated elevation of CBF was significantly reduced by single administration of TPM (Figure 7). Negative deflection of DC potential only at the proximal site but not at the distal site, with or without a small CBF change, was detected in five rats after TPM administration. Physiological parameters (MABP, HR, arterial pH, partial pressure of arterial oxygen (PaO_2) and carbon dioxide ($PaCO_2$)) were within normal ranges and were not significantly changed either by KCl application or by intragastric administration of TPM (Table 2).

Discussion

In our study, chronic peroral administration of TPM suppressed CSD susceptibility, whereas single administration had little effect on CSD susceptibility. Intraperitoneal administration of TPM for 4 weeks suppressed CSD occurrence frequency induced by KCl application, enhanced the cathodal stimulation threshold and lowered the propagation speed, and longer administration (17 weeks) almost abolished CSD occurrence (23). Thus, oral administration for a longer period would be expected to have a potent effect on CSD susceptibility.

The administered amount and plasma concentration of TPM in the present experiment were much higher than the clinically used levels in human. We demonstrated rapid and stable absorption of orally administered TPM in this study. However, the TPM concentration before the final administration was very low in this experiment, indicating that TPM was largely eliminated within 1 day in rats, and no accumulation effect was observed during daily administration for 6 weeks. The biological half-life ($T_{1/2}$) in humans is 27–31 h (24). Thus, species difference in TPM turnover rate and/or bioavailability might require a higher dose in rats, and drug accumulation might also be different. We found that CSD occurrence and propagation before the final dose of TPM in the 6-week daily administration protocol were not different from those of the vehicle control. This suggests that there might be a drug threshold of approximately 25 μg/ml in rats. This in turn might be consistent with the observation in the PROMPT trial that cessation of chronic TPM resulted in loss of the prophylactic effect (25), and suggests that monitoring of plasma TPM levels might be important for effective treatment.

Single gavage administration of TPM had no effect on CSD susceptibility in our experiment. It was also reported by others that single intraperitoneal administration did not reduce the number of CSD episodes induced by KCl (23). These facts may suggest that a certain period is required for manifestation of the prophylactic effect of TPM. However, a single dose of intravenous TPM inhibited CSD occurrence induced by needle plunge, but did not influence the CSD propagation speed in anesthetized rats and cats (20). One possible explanation might be a time lag in the transfer of TPM from blood to brain. It is also possible that there is a depot effect due to drug accumulation within a sequestered brain compartment. Although it is possible that a single dose might block propagation in the distal direction as seen in our experiment, a similar phenomenon was also seen in chronically treated rats. CSD seems to be more effectively suppressed by chronic treatment. Although intravenous injection might provide rapid relief of migraine, it may be possible to

obtain a long-lasting prophylactic effect in humans by regular intragastric administration, which is a more convenient route.

It was reported that chronic intraperitoneal administration of TPM dose-dependently suppressed CSD susceptibility, though the dosages (40–80 mg/kg/day) were lower than in our study (23). It should be borne in mind that the administration methods were different; intraperitoneal administration in previous studies and oral gavage in our experiment. We found that the maximum plasma level after intraperitoneal administration was approximately three times that after intragastric administration. It seems possible that intragastric administration may result in lower TPM blood levels because of restricted absorption at the gastrointestinal tract, but it may allow the blood level of TPM to be maintained for a longer period, than with intraperitoneal administration. Thus, higher doses may be required in the case of intragastric administration.

CBF elevation related to potassium-evoked CSD was not affected by chronic TPM treatment, whereas it was suppressed by single administration of TPM in our study. This effect of single administration is consistent with that described previously (20). The mechanism of vasodilation associated with CSD is complicated, being influenced by multiple stimuli arising from cerebral arteries and parenchyma, including various neurotransmitters secreted by sensory and parasympathetic nerves (26). TPM diminished neurogenic dural vasodilation by inhibiting the presynaptic release of calcitonin gene-related peptide (CGRP) from trigeminal neurons, but did not act postsynaptically at blood vessels (27). A single dose of TPM might attenuate vasodilation by reducing release of vasodilative substances, such as CGRP, whereas the suppressive response might be attenuated and/or compensated for by other mechanisms in the chronically treated rats.

TPM has been reported to suppress excitatory amino-acid-related synaptic transmission and ion channels (28,29). Conversely, the drug enhances $GABA_A$ receptor-mediated inhibitory currents and blocks the GluK1 agonist-mediated suppression of GABA release from interneurons (30). Although it has not been demonstrated that GABA receptors directly modulate CSD susceptibility, it is possible that TPM might suppress CSD occurrence and propagation via interference with excitatory amino-acid-mediated ion channels and/or inhibition of GABA-mediated depolarization.

In our study, we used daily administration of TPM for 6 weeks, so it is possible that the suppressive effect of TPM on CSD involves induction of enzyme/receptor(s) or modulation of gene expression. TPM enhanced GABA release by down-regulation of $GABA_B$ autoreceptor expression and up-regulation of astroglial TWIK-related acid-sensitive K^+ channel-1 in gerbils (31,32). A neuroprotective effect of TPM was seen as an enhancement of cell survival on exposure of primary neuronal-astroglial cultures to glutamate- and kainate-induced neurotoxicity (33) and blockade of up-regulation of caspase-3 expression in hippocampus of kindled rats (34). These results suggest a possible mechanism of the antiepileptic effects of TPM. A similar mechanism may be involved for migraine. Thus, chronic TPM treatment may induce up- or down-regulation of certain neuronal and/or astroglial proteins, leading to suppression of neuronal activity associated with CSD and resulting in relief of migraine and/or aura.

Another migraine preventive drug, lamotrigine, had a potent suppressive effect on CSD susceptibility (especially CSD occurrence frequency) and c-Fos expression in the cortex, but did not affect propagation velocity (35). Lamotrigine is clinically effective on migraine with aura, but not on migraine without aura. On the other hand, migraine without aura as well as with aura was relieved by TPM in the clinical trial (17). The relieving effect of TPM on migraine might involve not only a decrease in CSD susceptibility, but also other mechanisms.

Conclusion

Chronic treatment with TPM suppressed CSD occurrence and propagation along the cerebral cortex, and is therefore expected to relieve migraine. However, continuous maintenance of a sufficient blood level of TPM appears to be necessary.

Acknowledgements

The authors thank Janssen Pharmaceutical K.K. for measurement of plasma concentration of TPM and generous support.

Funding

This work was supported by Grants-in-Aid for Scientific Research No. 22390182 (to NS) and No. 21591119 (to YT) from the Ministry of Education, Culture, Sports, Science and Technology of Japan, and by Janssen Pharmaceutical K.K.

Conflict of interests

The authors declare that there is no conflict of interest.

References

1. Goadsby PJ, Lipton RB and Ferrari MD. Migraine–current understanding and treatment. *N Engl J Med* 2002; 346: 257–270.
2. Katsarava Z, Fritsche G, Muessig M, Diener HC and Limmroth V. Clinical features of withdrawal headache following overuse of triptans and other headache drugs. *Neurology* 2001; 57: 1694–1698.

3. Iadecola C. From CSD to headache: a long and winding road. *Nat Med* 2002; 8: 110–112.
4. Moskowitz MA. Genes, proteases, cortical spreading depression and migraine: impact on pathophysiology and treatment. *Funct Neurol* 2007; 22: 133–136.
5. Leão A. Spreading depression of activity in cerebral cortex. *J Neurophysiol* 1944; 7: 359–390.
6. Lauritzen M. Pathophysiology of the migraine aura. *The spreading depression theory*. Brain 1994; 117: 199–210.
7. Bolay H, Reuter U, Dunn AK, Huang Z, Boas DA and Moskowitz MA. Intrinsic brain activity triggers trigeminal meningeal afferents in a migraine model. *Nat Med* 2002; 8: 136–142.
8. Ayata C. Spreading depression: from serendipity to targeted therapy in migraine prophylaxis. *Cephalalgia* 2009; 29: 1095–1114.
9. Richter F, Mikulik O, Ebersberger A and Schaible HG. Noradrenergic agonists and antagonists influence migration of cortical spreading depression in rat-a possible mechanism of migraine prophylaxis and prevention of postischemic neuronal damage. *J Cereb Blood Flow Metab* 2005; 25: 1225–1235.
10. Shank RP, Gardocki JF, Streeter AJ and Maryanoff BE. An overview of the preclinical aspects of topiramate: pharmacology, pharmacokinetics, and mechanism of action. *Epilepsia* 2000; 41(Suppl 1): S3–S9.
11. Diener HC, Bussone G, Van Oene JC, Lahaye M, Schwalen S, Goadsby PJ, et al. Topiramate reduces headache days in chronic migraine: a randomized, double-blind, placebo-controlled study. *Cephalalgia* 2007; 27: 814–823.
12. Diener HC, Tfelt-Hansen P, Dahlof C, Lainez MJ, Sandrini G, Wang SJ, et al. Topiramate in migraine prophylaxis–results from a placebo-controlled trial with propranolol as an active control. *J Neurol* 2004; 251: 943–950.
13. Silberstein SD, Lipton RB, Dodick DW, Freitag FG, Ramadan N, Mathew N, et al. Efficacy and safety of topiramate for the treatment of chronic migraine: a randomized, double-blind, placebo-controlled trial. *Headache* 2007; 47: 170–180.
14. Brandes JL, Saper JR, Diamond M, Couch JR, Lewis DW, Schmitt J, et al. Topiramate for migraine prevention: a randomized controlled trial. *JAMA* 2004; 291: 965–973.
15. Dodick DW, Silberstein S, Saper J, Freitag FG, Cady RK, Rapoport AM, et al. The impact of topiramate on health-related quality of life indicators in chronic migraine. *Headache* 2007; 47: 1398–1408.
16. Lofland JH, Gagne JJ, Pizzi LT, Rupnow M and Silberstein SD. Impact of topiramate migraine prophylaxis on workplace productivity: results from two US randomized, double-blind, placebo-controlled, multicenter trials. *J Occup Environ Med* 2007; 49: 252–257.
17. Reuter U, Del Rio MS, Diener HC, Allais G, Davies B, Gendolla A, et al. Migraines with and without aura and their response to preventive therapy with topiramate. *Cephalalgia* 2010; 30: 543–551.
18. Sanchez-Del-Rio M, Reuter U and Moskowitz MA. New insights into migraine pathophysiology. *Curr Opin Neurol* 2006; 19: 294–298.
19. Ayata C. Cortical spreading depression triggers migraine attack: pro. *Headache* 2010; 50: 725–730.
20. Akerman S and Goadsby PJ. Topiramate inhibits cortical spreading depression in rat and cat: impact in migraine aura. *Neuroreport* 2005; 16: 1383–1387.
21. Unekawa M, Tomita M, Tomita Y, Toriumi H and Suzuki N. Sustained decrease and remarkable increase of red blood cell velocity in intraparenchymal capillaries associated with potassium-induced cortical spreading depression in rats. *Microcirculation* 2012; 19: 166–174.
22. Goswami D, Kumar A, Khuroo AH, Monif T and Rab S. Bioanalytical LC-MS/MS method validation for plasma determination of topiramate in healthy Indian volunteers. *Biomed Chromatogr* 2009; 23: 1227–1241.
23. Ayata C, Jin H, Kudo C, Dalkara T and Moskowitz MA. Suppression of cortical spreading depression in migraine prophylaxis. *Ann Neurol* 2006; 59: 652–661.
24. Bahrami G, Mirzaeei S and Kiani A. Sensitive analytical method for Topiramate in human serum by HPLC with pre-column fluorescent derivatization and its application in human pharmacokinetic studies. *J Chromatogr B Analyt Technol Biomed Life Sci* 2004; 813: 175–180.
25. Diener HC, Agosti R, Allais G, Bergmans P, Bussone G, Davies B, et al. Cessation versus continuation of 6-month migraine preventive therapy with topiramate (PROMPT): a randomised, double-blind, placebo-controlled trial. *Lancet Neurol* 2007; 6: 1054–1062.
26. Busija DW, Bari F, Domoki F, Horiguchi T and Shimizu K. Mechanisms involved in the cerebrovascular dilator effects of cortical spreading depression. *Prog Neurobiol* 2008; 86: 379–395.
27. Akerman S and Goadsby PJ. Topiramate inhibits trigeminovascular activation: an intravital microscopy study. *Br J Pharmacol* 2005; 146: 7–14.
28. Poulsen CF, Simeone TA, Maar TE, Smith-Swintosky V, White HS and Schousboe A. Modulation by topiramate of AMPA and kainate mediated calcium influx in cultured cerebral cortical, hippocampal and cerebellar neurons. *Neurochem Res* 2004; 29: 275–282.
29. Zona C, Ciotti MT and Avoli M. Topiramate attenuates voltage-gated sodium currents in rat cerebellar granule cells. *Neurosci Lett* 1997; 231: 123–126.
30. Braga MF, Aroniadou-Anderjaska V, Li H and Rogawski MA. Topiramate reduces excitability in the basolateral amygdala by selectively inhibiting GluK1 (GluR5) kainate receptors on interneurons and positively modulating $GABA_A$ receptors on principal neurons. *J Pharmacol Exp Ther* 2009; 330: 558–566.

31. Kim DS, Kim JE, Kwak SE, Choi HC, Song HK, Kimg YI, et al. Up-regulated astroglial TWIK-related acid-sensitive K^+ channel-1 (TASK-1) in the hippocampus of seizure-sensitive gerbils: a target of anti-epileptic drugs. *Brain Res* 2007; 1185: 346–358.
32. Kim DS, Kwak SE, Kim JE, Won MH, Choi HC, Song HK, et al. The effect of topiramate on GABA(B) receptor, vesicular GABA transporter and paired-pulse inhibition in the gerbil hippocampus. *Neurosci Res* 2005; 53: 413–420.
33. Ängehagen M, Ben-Menachem E, Rönnbäck L and Hansson E. Topiramate protects against glutamate- and kainate-induced neurotoxicity in primary neuronal-astroglial cultures. *Epilepsy Res* 2003; 54: 63–71.
34. Chen X, Bao G, Hua Y, Li Y, Wang Z and Zhang X. The effects of topiramate on caspase-3 expression in hippocampus of basolateral amygdala (BLA) electrical kindled epilepsy rat. *J Mol Neurosci* 2009; 38: 201–206.
35. Bogdanov VB, Multon S, Chauvel V, Bogdanova OV, Prodanov D, Makarchuk MY and Schoenen J. Migraine preventive drugs differentially affect cortical spreading depression in rat. *Neurobiol Dis* 2011; 41: 430–435.

Microcirculation
The Official Journal of the Microcirculatory Society, Inc. and the British Microcirculation Society

DOI:10.1111/j.1549-8719.2011.00143.x

Original Article

Sustained Decrease and Remarkable Increase in Red Blood Cell Velocity in Intraparenchymal Capillaries Associated With Potassium-Induced Cortical Spreading Depression

MIYUKI UNEKAWA, MINORU TOMITA, YUTAKA TOMITA, HARUKI TORIUMI, AND NORIHIRO SUZUKI

Department of Neurology, School of Medicine, Keio University, Shinjuku-ku, Tokyo, Japan
Address for correspondence: Miyuki Unekawa, Department of Neurology, School of Medicine, Keio University, 35 Shinanomachi, Shinjuku-ku, Tokyo 160-8582, Japan. *E-mail:* unekawa.m@z5.keio.jp

Received 19 July 2011; accepted 8 October 2011.

ABSTRACT

Objectives: To examine changes in red blood cell (RBC) velocity in intraparenchymal capillaries of rat cerebral cortex in response to KCl-induced cortical spreading depression (CSD).

Methods: In isoflurane-anesthetized rats, the velocity of fluorescently labeled RBCs flowing in capillaries in layer I was measured with a high-speed camera laser-scanning confocal fluorescence microscope, with simultaneous monitoring of DC potential, the electroencephalogram (EEG), partial pressure of oxygen (PO_2), and cerebral blood flow (CBF).

Results: After KCl application, a transient deflection of DC potential (i.e., CSD) repeatedly appeared concomitantly with depression of EEG, and was propagated in the distal direction. PO_2 transiently decreased and CBF was slowly elevated. The frequency distribution of RBC velocity was shifted downward during CSD and was still low after the passage of CSD. When we observed RBC velocity in 38 individual capillaries, 10 capillaries exhibited slowed-down RBC during CSD and RBC velocity remained low in 2 even after the passage of CSD. On the other hand, RBCs with moderately (<3 mm/sec) or remarkably (>3 mm/sec) increased velocities were seen in 10 and 5 capillaries, respectively.

Conclusion: CSD-induced excitation of neurons may sustainably decrease or greatly increase RBC velocity in capillaries.

Key words: confocal fluorescence microscopy, cortical spreading depression, neuro-capillary coupling, red blood cell velocity, thoroughfare channel

Abbreviations used: ABP, arterial blood pressure; CBF, cerebral blood flow; CSD, cortical spreading depression; DC, direct current; EEG, electroencephalogram; FITC, fluorescent isothiocyanate; LDF, laser Doppler flowmeter; MABP, mean arterial blood pressure; PO_2, partial tissue pressure of oxygen; RBC, red blood cell.

Please cite this paper as: Unekawa M, Tomita M, Tomita Y, Toriumi H and Suzuki N. Sustained Decrease and Remarkable Increase in Red Blood Cell Velocity in Intraparenchymal Capillaries Associated With Potassium-Induced Cortical Spreading Depression. *Microcirculation* **19:** 166–174, 2012.

INTRODUCTION

CSD is a phenomenon involving mass depolarization of neurons and glial cells, followed by sustained suppression of spontaneous neuronal activity [14]. It is accompanied by various changes in blood flow and energy metabolism [6], and is thought to be involved in the mechanisms of various pathological conditions, such as migraine [12]. CSD has been experimentally elicited with a variety of chemical, electrical and mechanical stimuli in various animals, and research in animal models has provided information about its pathological role, as well as clues to potential clinical therapies. Artificially evoked CSD spreads through the cortical tissue from the initiation site toward the periphery at a rate of 2–5 mm/min, with suppression of the EEG [3], deflection of DC potential, and repetitive changes in light transmission [31]. CSD induces marked increases in glucose utilization and metabolism in the cerebral cortex [21], and the cerebral metabolic rate of oxygen shows a prolonged increase [18]. This elevation of oxygen consumption often leads to tissue hypoxia [25], and changes in PO_2 elicited by CSD are closely linked to CBF changes [11].

The response of CBF to CSD is complex, being mediated by the production and release of multiple vasodilating and vasoconstricting factors by diverse cells within the neurovascular unit [5]. Although it is accepted that hyperemia during CSD is followed by a long-lasting reduction to

below the prestimulus level [13], some findings are not necessarily consistent with this, especially with respect to vasoconstrictive response [3,8,10,15,16].

Various flow control systems of cerebral vessels serve to supply blood to the capillaries at levels sufficient to meet local neuronal requirements. RBC behavior in capillaries is especially important, as RBCs are the predominant oxygen carrier from the lung to the tissue. We have reported the detection of high-velocity RBCs in urethane-anesthetized rats, using a high-speed camera laser-scanning confocal fluorescence microscope system with Matlab-domain tracking software, KEIO-IS2, developed by us [19,27,33]. We found that RBC velocity in intraparenchymal capillaries was often independent of upstream arteriolar blood flow or tissue perfusion in the surrounding microvasculature. When local CBF was dramatically increased by topical application of nitric oxide on the brain surface, "microflow" in capillaries was rather decreased, while "RBC velocity" remained unchanged [28]. "RBC flow" in capillaries seems to be actively controlled in response to neuronal requirements, that is, there appears to be a neuro-capillary coupling [32].

The nature of RBC flow change during CSD is still controversial; reports have indicated an increase in adult mice [25], a drop and cessation of flow in neonatal rats [7], and a decrease in adult rats [30,32]. In this study, to examine the influence of neuronal activity on RBC velocity in nearby capillaries in terms of the neuro-capillary coupling hypothesis, we evaluated electrophysiological changes, tissue level of oxygen and CBF simultaneously with measurement of RBC velocity in capillaries in response to potassium-induced CSD.

MATERIALS AND METHODS

General Procedures

Animals were used with the approval (No. 09058) of the Animal Ethics Committee of Keio University (Tokyo, Japan), and all experimental procedures were in accordance with the university's guidelines for the care and use of laboratory animals. Male Sprague–Dawley rats (CLEA Japan, Inc., Tokyo, Japan) (10–15 weeks, $n = 26$) were anesthetized with isoflurane (2.5–3.0% in room air with flow rate of 250 mL/min) via a concentration-controllable anesthesia unit (400; Univentor Ltd., Zejtun, Malta). Body temperature was maintained with a heating-pad and thermo-controller (BWT-100; Bioresearch Center Co., Ltd., Nagoya, Japan). Each rat was fixed to a head-holder (SG-4N, modified to be flexible around the horizontal axis; Narishige Scientific Instrument Laboratory, Tokyo, Japan) and a cranial window of approximately 4 mm in diameter was opened in the left side of the skull at the parieto-temporal region of the cerebral cortex. The dura was carefully removed and the exposed cortex was covered with a coverslip to prevent it from drying out. CSD was induced by applying a drop (5 μL) of 1.0 M KCl solution into an additional posterior hole of 2 mm in diameter having its center at the coordinates of 7 mm posterior and 2 mm lateral to the bregma. ABP was continuously recorded through a femoral arterial catheter via a surgical strain-gage (MLT0670 and ML117; ADInstruments Pty. Ltd., Bella Vista, NSW, Australia). KCl solution was administered after confirmation that all parameters had remained stable for at least 10 minutes. Animals in which all parameters were still stable at more than 30 minutes after the last CSD episode were given a further application of KCl solution.

Measurement of PO_2 and CBF

An oxygen electrode (POE-10N; Bioresearch Center Co., Ltd.) with a tip diameter of 200 μm was inserted 300 μm under the pia mater at the coordinates of 2 mm posterior and 0.5 mm lateral to the bregma (medial edge of the cranial window) and fixed with dental cement (see Figure 1). A reference electrode (POR-10N; Bioresearch Center Co., Ltd.) was placed subcutaneously in the back. PO_2 was continuously monitored with an oxygen monitor (PO2-100DW; Inter Medical Co., Ltd., Nagoya, Japan). CBF was monitored with a laser Doppler flowmeter (LDF, ALF 21R; Advance Co., Ltd., Tokyo, Japan). The probe, having a diameter of 0.8 mm, was placed on the surface of the cortex at the coordinates of 2 mm posterior and 4 mm lateral to the bregma (lateral edge of the cranial window; see Figure 1).

Measurement of DC Potential and EEG

Two Ag/AgCl electrodes (tip diameter = 200 μm, EEG-5002Ag; Bioresearch Center Co., Ltd.) were inserted

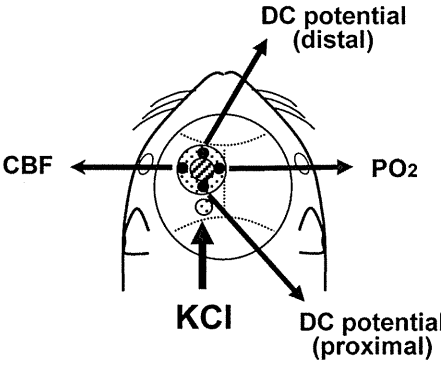

Figure 1. Positioning of electrodes for DC potential and EEG measurement, an electrode for PO_2, and an LDF probe in the cranial window. Flow of FITC-labeled RBCs was recorded with a high-speed camera laser-scanning confocal fluorescence microscope at the center of the cranial window as shown by a dotted circle. KCl solution was administered into the posterior burr hole.

200 μm under the pia mater at the anterior edge (0.5 mm posterior and 2 mm lateral to the bregma) and posterior edge (3.5 mm posterior and 2 mm lateral to the bregma) of the cranial window, and fixed with dental cement (see Figure 1). The locations of the electrodes and the probe were sometimes slightly moved to avoid a large vessel. Ag/AgCl reference electrodes (EER-5004Ag; Bioresearch Center Co., Ltd.) were subcutaneously placed in the space between the skull-bone and the scalp. DC potential was amplified at 1–100 Hz and digitized at 1 kHz with a differential headstage and differential extracellular amplifier (Model 4002 and EX1; Dagan Co., Minneapolis, MN, USA). The signal of DC potential was further digitally filtered with a 5 Hz low cut, to minimize the basal fluctuation due to heart rate and breathing, to obtain the EEG.

Analysis of RBC Velocity

FITC-labeled RBC suspension, prepared beforehand according to Seylaz *et al.* [20], was injected into the bloodstream through the venous catheter so that the final percentage of FITC-labeled RBCs/total RBCs in the circulating blood was approximately 0.4%. The velocity of FITC-labeled RBCs was automatically calculated using the high-speed camera (500 fps) laser-scanning confocal fluorescence microscope and the image analyzing system with MATLAB (The MathWorks, Inc., Natick, MA, USA) environment application software (KEIO-IS2) developed in our laboratory [19], as reported elsewhere [27]. The images acquired with the high-speed system could be recorded only for up to 15 seconds due to the limitation of file size (2 GB) in our analysis system. With reference to the alternatively recorded images obtained using a conventional video camera, we discriminated single capillaries from other vessels such as arterioles and venules, by using the criterion that capillaries should have a diameter of <10 μm [9,35]. The frequency distribution was obtained by classification of velocities in steps of 0.5 mm/sec and counting the RBCs within each step [33].

Data Analysis

ABP, PO_2, CBF, DC potential, and EEG were recorded continuously. The data were stored on a multichannel recorder (PowerLab 8/30; ADInstruments Pty. Ltd.) and analyzed off-line with LabChart software (ADInstruments Pty. Ltd.). The time courses of the responses of PO_2, CBF, and DC potential were determined by taking time zero as the point at which the DC potential at the proximal portion began to decrease. The trough and peak of PO_2, the peak of CBF, and the trough of DC potential were estimated. CSD duration was estimated as the period till the recovery rate became minimal. The response and delay times of the parameters were determined for each CSD episode, and were averaged for each application of KCl. CSD propagation speed was calculated based on the time and the distance between the two recording electrodes. ABP was averaged for one minute before and for every 15 seconds after the beginning of deflection of DC potential at the proximal portion. Post-CSD oligemia was evaluated as the average of the minimum CBF after the last CSD episode elicited by a single application of KCl.

Statistical comparison of RBC velocities between different periods was performed with nonparametric multiple comparison (Games–Howell test) after confirmation of homogeneity of variance with one-way ANOVA (Kruskal–Wallis test). Statistical comparison of two groups was performed with Student's *t*-test. Average data are presented as mean ± SD and a *p*-value of <0.05 was considered to be statistically significant.

RESULTS

General Results

The body weight of the rats was 402 ± 83 g. The initial level of MABP was 77 ± 11 mmHg. MABP was maintained within ±20 mmHg in each rat throughout the experiments, and did not decrease below 60 mmHg in any rat.

As shown in Figure 2A, one application of KCl induced repetitive (between 3 and 16 times) negative deflections of DC potential (i.e., CSD). CSD was detected first at the posterior (proximal) portion, and then at the anterior (distal) portion with a delay time of 27 to 110 seconds. Every CSD episode was accompanied by a long-lasting decrease in EEG amplitude, occasionally preceded by a transient increase. As CSD occurred, PO_2 transiently declined, followed by a slight increase, while CBF slowly increased, then returned toward the baseline. MABP was constant during repetitive CSD after KCl application, namely, the CBF responses were locally elicited, not due to change in systemic blood pressure.

Occasionally, unusual responses were observed. In four applications of KCl among 25 applications for which all parameters were successfully measured, CBF was transiently decreased, followed by a slight increase to above the baseline during CSD, as shown in Figure 2B. In seven rats, oppositely propagated CSD was found, namely CSD was detected first at the anterior (distal) portion and then detected at the posterior (proximal) portion, as illustrated in Figure 2B (second episode of CSD). In total, 11 episodes of CSD out of 162 were oppositely propagated with a time difference of 59.5 ± 56.0 seconds (vs 55.5 ± 28.2 seconds for forward propagated episodes in the same rats). Such CSD was observed only after the second or a later episode in the series of CSD episodes induced by a single KCl application.

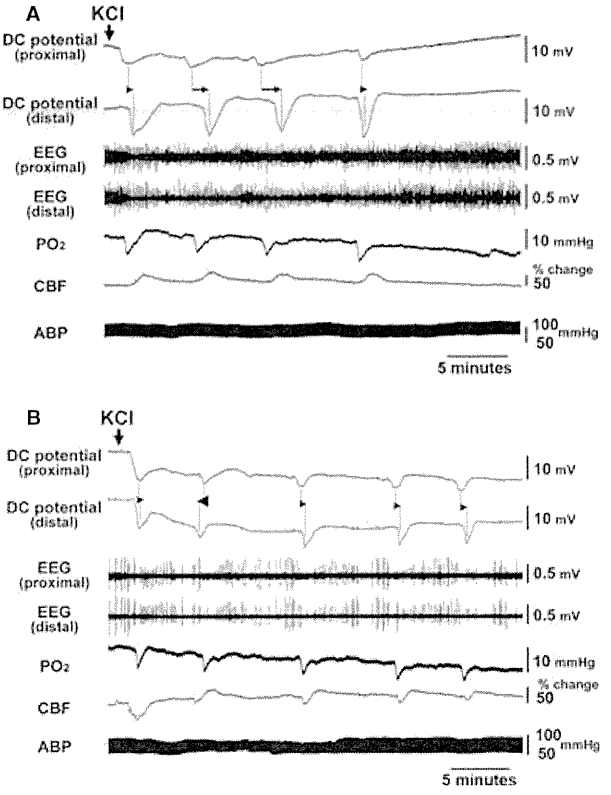

Figure 2. Changes in DC potential, EEG, PO_2, CBF, and ABP in response to KCl application. Typical signals are shown in (**A**). DC potential deflection detected at the proximal portion propagated to the distal portion, as shown with arrows. Occasionally, CBF showed a transient decrease, followed by a slight increase during CSD, and/or DC potential deflection was detected first at the distal portion, as shown with the reversed arrowhead (**B**).

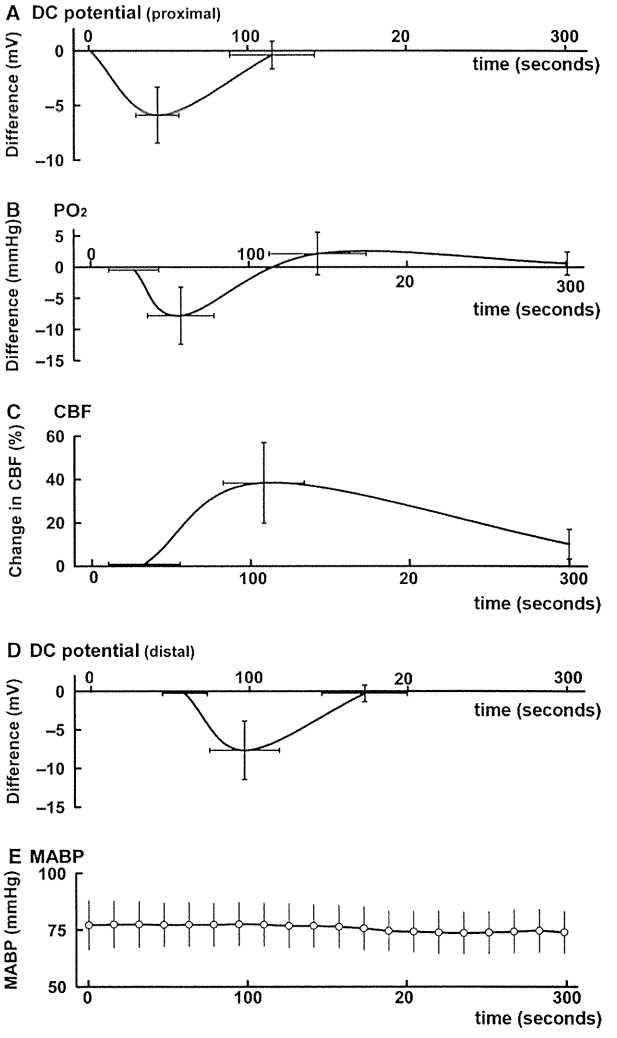

Figure 3. Average response curves of DC potential (proximal portion, **A** and distal portion, **D**), PO_2 (**B**), CBF (**C**), and MABP (**E**) following KCl application. The onset of the DC potential suppression at the proximal portion was defined as time zero. Values of delay time and peak changes are mean ± SD and points were connected with a smooth curve (**A**–**D**). ABP was averaged over every 15 seconds in each rat and plotted as mean ± SD (**E**).

Physiological and Electrophysiological Responses to CSD

On average, 6.5 ± 3.2 episodes of CSD were elicited by one application of KCl. The averages of the responses and delay times of the parameters in 21 applications of KCl in 14 rats are summarized in Figure 3. First, deflection of DC potential at the posterior (proximal) portion was detected (Figure 3A). Secondly, PO_2 began to decrease with a delay of 27.6 ± 15.7 seconds and reached the lowest level (−7.4 ± 3.6 mmHg), followed by a slight increase (+2.6 ± 3.8 mmHg) (Figure 3B). CBF began to increase with a delay of 33.5 ± 22.4 seconds, reached the highest level (+38.5 ± 18.6%) at a time 1.83 times longer than in the case of DC potential deflection, and then gradually declined to the baseline (Figure 3C). Finally, deflection of DC potential was detected at the anterior (distal) portion with a delay time of 54.6 ± 22.1 seconds (Figure 3D). Propagation speed from the proximal to the posterior side was calculated as 3.3 ± 1.3 mm/min according to the distance between the electrodes. MABP did not change for five minutes after CSD elicitation (Figure 3E). Post-CSD oligemia was not observed in this experiment, as indicated by the minimum CBF after the last CSD episode (+5.9 ± 21.1%).

Change in RBC Velocity in Capillaries

Confocal microscopic movies for the analysis of RBC velocity were recorded for 10–15 seconds at representative periods, before KCl application (Before-KCl), just after the trough of DC potential deflection at the proximal portion was detected (Intra-CSD), between CSD when all parameters

had returned to the baseline (Inter-CSD), and approximately one hour after KCl application, when CSD had ceased (After-CSD), as shown in Figure 4A. In the Intra-CSD period, DC potential at the center of the cranial window was presumed to be included within the negative deflection according to the time course of the response (Figure 3).

For each recording period, we obtained the frequency distribution as defined in Materials and Methods. In the Before-KCl period, the mean RBC velocity was 2.02 ± 1.58 mm/sec for 551 detected RBCs (12 rats, total recording time 176 seconds). RBC velocities peaked at around 1.0–2.0 mm/sec, but showed tailing to higher velocities, up to 9.3 mm/sec; 66% of the velocity values lay within the range of 0.5–2.0 mm/sec (Figure 4B). These results are comparable to those in our previous report [33]. In the Intra-CSD period, mean RBC velocity was 1.95 ± 1.80 mm/sec for 802 detected RBCs (12 rats, total recording time 353 seconds). The frequency distribution apparently shifted downward with a reduction in the number of RBCs having a velocity of around 2 mm/sec. Unexpectedly, velocity remained low in the Inter-CSD period, even though CBF and other parameters had returned to the baseline, and the average (1.64 ± 1.52 mm/sec for 562 RBCs in 10 rats, total recording time 206 seconds) was significantly lower than in the Before-KCl period ($p < 0.01$) and the frequency distribution tended to retain its downward shift. The velocity recovered in the After-CSD period (2.18 ± 1.31 mm/sec for 232 RBCs in nine rats, total recording time 188 seconds). Throughout the Intra- and Inter-CSD periods, RBCs with velocities higher than 3 mm/sec remained, but RBCs with velocities lower than 3 mm/sec showed an apparent shift toward slower velocities.

Next, we evaluated RBC velocity in a single capillary for each record period. Capillaries in which moving RBCs were detected both before and after KCl application were picked up from the velocity data (38 capillaries in total). The changes are plotted in Figure 5A–C. RBC velocity in 10 capillaries decreased in the Intra-CSD period (Figure 5A). Within such capillaries, RBC velocity in two capillaries remained low even after passage of CSD, as indicated by arrows, whereas other capillaries showed full or partial recovery of RBC velocity. In contrast, RBC velocity in 20 capillaries increased in the Intra-CSD period. Among the capillaries with accelerated RBCs, we found 15 capillaries in

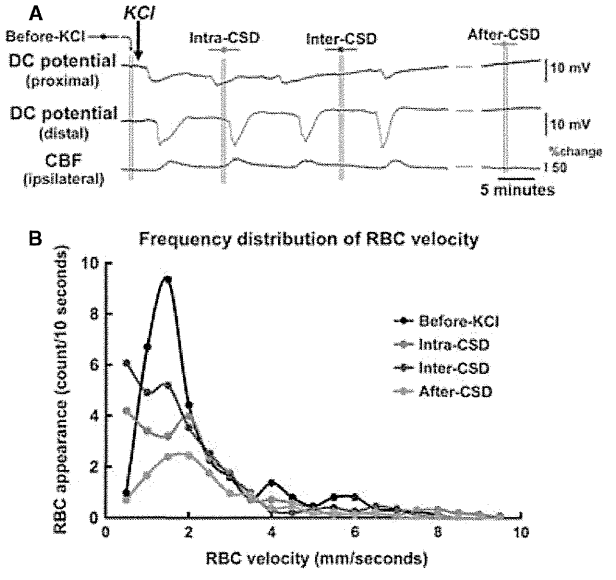

Figure 4. Analysis results of RBC velocities in capillaries. The motion pictures using the high-speed camera laser-scanning confocal fluorescence microscope were obtained at the times shown in (**A**); before KCl application (Before-KCl; black circle and line), just after the trough of DC potential deflection at the proximal portion was detected (Intra-CSD; red circle and line), several minutes after the DC potential at both portions had recovered (Inter-CSD; blue circle and line) and at one hour after KCl application (After-CSD; green circle and line). (**B**) Frequency distribution of RBC velocities in single capillaries in which the velocities of detected RBCs were counted for every 0.5 mm/sec step and RBC appearance per 10 seconds were plotted.

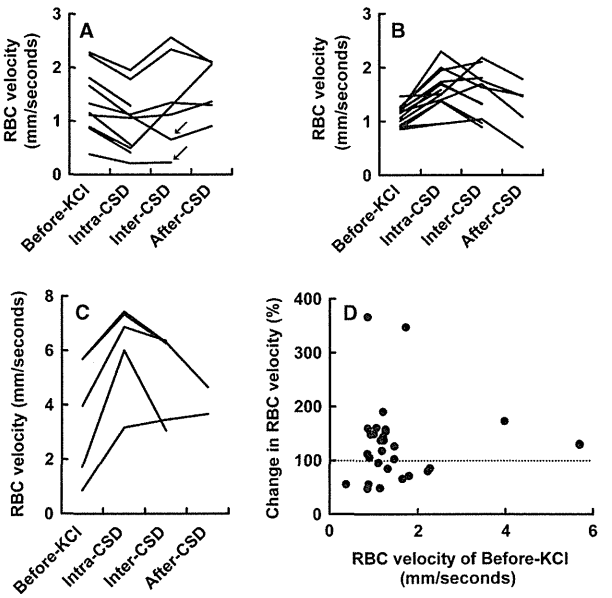

Figure 5. Profiles of RBC velocity in 30 capillaries: plotted for the Before-KCl, Intra-CSD, Inter-CSD, and After-CSD periods. (**A**) RBC velocity in 10 capillaries decreased in the Intra-CSD period. Velocity in two capillaries was still low after passage of CSD (Inter-CSD period) as indicated by arrows. (**B**) Increase in RBC velocity in 15 capillaries in the Intra-CSD period, in which velocity did not exceed 3 mm/sec. (**C**) RBC velocity in five capillaries was remarkably increased (>3 mm/sec) in the Intra-CSD period. (**D**) Scatter diagram of change in RBC velocity in the Intra-CSD period versus the velocity within the identical capillary before KCl application.

which RBC velocity did not exceed 3 mm/sec (Figure 5B) and five capillaries in which RBC velocity was remarkably increased (>3 mm/sec), then returned toward the basal level (Figure 5C). In eight capillaries, moving RBCs could not be detected in the Intra-CSD period, but appeared after CSD passage (Inter-CSD; data not shown). Next, we calculated RBC velocity changes from the period of Before-KCl to Intra-CSD. There was no correlation between basal velocity in the Before-KCl period and velocity change between the period of Before-KCl and Intra-CSD (Figure 5D).

Furthermore, moving RBCs were followed in a certain ROI and tracked with KEIO-IS2 (Figure 6). Capillaries with slowed-down RBCs and those with accelerated RBCs did not appear to be confined to any specific location, but rather were located together in similar regions. The five capillaries in which RBC velocity was greatly increased in the Intra-CSD period (Figure 5C) were all straight; an example is shown with a green solid arrow in Figure 6A.

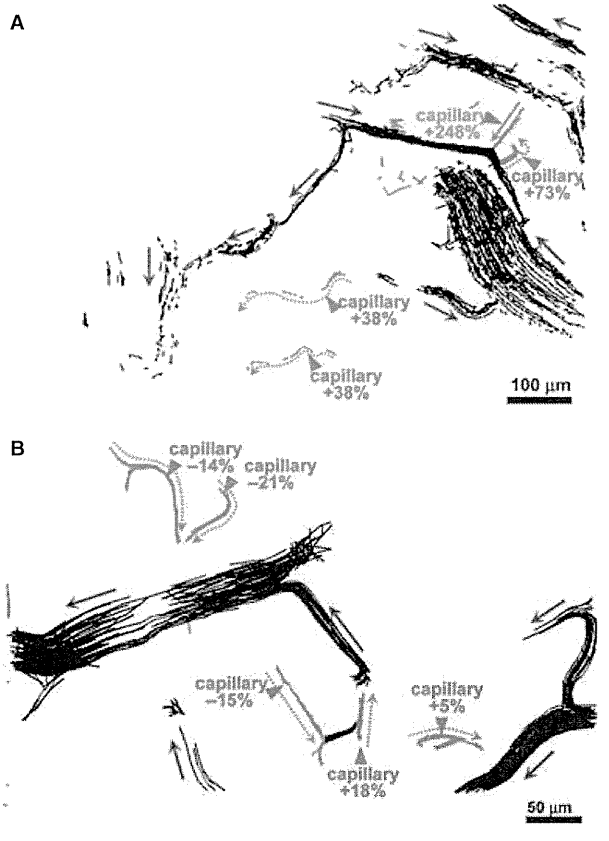

Figure 6. RBC tracking map indicating RBC movement in various vessels. These maps were calculated with KEIO-IS2 from 5000 frames (10 seconds) obtained with the high-speed camera laser-scanning confocal fluorescence microscope in different rats (**A**, **B**). RBC tracks flowing in capillaries are highlighted in red. RBC flow direction in major veins and venules is indicated with blue arrows. Capillaries in which RBC velocities could be calculated in both the Before-KCl and Intra-CSD periods are shown with the velocity changes (%), with the flow direction indicated by green dotted arrows. Greatly accelerated RBCs in a capillary are shown with green letters and a green solid arrow (**A**).

DISCUSSION

CSD-Induced Changes in Metabolism and CBF

MABP of the rats appears to be slightly low, possibly due to the effect of anesthesia, but the values of all rats were within the range of autoregulation and remained quite stable during experiments, so that cerebral circulation seems not to be substantially affected by ABP.

The response of cerebral metabolism to CSD has been well studied. As the wave of CSD passes, the cerebral metabolic rate is increased and the inadequate O_2 supply leads to stimulation of anaerobic glycolysis [10]. Significantly increased O_2 consumption is coupled to an augmentation of blood flow without change in O_2 extraction, suggesting that delivery of O_2 is not an important factor in the cerebral metabolic response to CSD [15]. The decrease in PO_2 which preceded the CBF response in our experiment appears to confirm that metabolic enhancement is due to potassium-induced neuronal activation, not due to the change in CBF.

On the other hand, PO_2 elevation seems to be dependent on CBF increase, as the CSD-induced elevation of PO_2 after transient hypoxia was roughly proportional to blood flow elevation [11], and regional CBF and PO_2 were simultaneously increased in response to CSD [36]. However, we recorded various parameters simultaneously and continuously with ipsilaterally fixed electrodes and probe. Thus, we have obtained convincing evidence that CSD facilitates energy metabolism, thereby consuming oxygen, and the regional hypoxia induces CBF elevation; furthermore, the subsequent elevation of PO_2 is at least partly due to CBF increase in our experiment.

Hypoperfusion After CSD

It has been reported that CSD elicits CBF increase followed by long-lasting decrease, namely post-CSD oligemia [8,13,38]. However, we did not observe prolonged hypoperfusion in our experiment. The reason for the difference is unclear, but may be related to differences in species, anesthesia, method of eliciting CSD, experimental conditions, and so on.

Initial transient hypoperfusion was seen in only three rats in this experiment. Brief hypoperfusion preceding hyperemia has already been reported [8,22,31]. The duration of initial hypoperfusion was correlated with the duration of the DC shift in rats [2]. Hypoxia and/or hypotension amplified the hypoperfusion and diminished the subsequent hyperemia after CSD [23]. A remarkable

initial decrease in CBF was reported to be associated with hypotension [24]. We did not find any correlation of initial hypoperfusion with the duration of the DC shift (92–146 vs 80–160 seconds in the group without hypoperfusion), with frequency of CSD occurrence (3–7 vs 3–16 times), with propagation speed (3.4–8.5 vs 1.6–6.5 mm/min), or with MABP (72 ± 1 vs 77 ± 11 mmHg). CSD-induced vasoconstriction seems to counteract vasodilation [5]. Initial vasoconstriction was observed both in rats and in mice, but the response was much larger in mice [2]. Overall, the vasoconstriction appeared to be suppressed under our experimental conditions, although it might be augmented in some cases.

Retrograde Propagation of CSD

Retrogradely propagated CSD was observed in 6.7% of CSD episodes in this experiment. Such CSD was found at the second or a later episode elicited by a single application of KCl. Approximately 40% of spreading depression waves penetrated through the amygdala into the caudate nucleus, and 70% of these waves returned to the cortex and spread through it toward the site of initiation, namely, a re-entry path for cortico-caudate-cortical propagation was demonstrated [34]. The ratio of the assumed return of CSD waves in our experiment was lower than that previously reported. We observed repetitive CSD in response to KCl application, whereas a single CSD wave was elicited with a small amount of KCl microinjection or electrical stimulation in the literature. The role of the basal ganglion in migraine remains unclear, but it must be involved in the pathogenesis of migraine. Indeed, cortically induced CSD evoked freezing behavior via activation of the amygdala, as indicated by enhancement of c-fos expression in the cerebral cortex and amygdala, in freely moving rats [1]. Increase in CSD due to reentry may result in enhancement of headache. Furthermore, it should be noted that cortico-caudate-cortical propagation may be influenced by external factors, such as stress, so that neuronal activity in the amygdala may be susceptible to modulation by various stimuli.

CBF and RBC Velocity

Theoretical O_2 extraction (E) at capillaries is dependent upon RBC velocity according to the classic Crone–Renkin equation: $E = 1 - e^{PS/f}$, where P is a constant related to the permeability, S corresponds to the capillary surface area, and f is the flow, which is linearly related to RBC velocity [26]. According to this relationship, a slower RBC velocity is more effective for exchange of O_2 between capillary and brain tissue. A transient increase in neuronal and/or glial activity associated with CSD may enhance the local capillary flow resistance, resulting in a reduction in RBC velocity [32]. Thus, a decrease in RBC velocity may enhance O_2 exchange efficiency to satisfy an increase in O_2 demand.

Examination of the effect of CSD on vascular function provides a means to explore the significance of neurovascular coupling under pathophysiological conditions. For this purpose, investigation of microcirculation, including capillary flow, seems to be effective. Line scanning by means of two-photon microscopy showed a prolonged period of increase in capillary flow, with a duration of up to several minutes, followed by a sustained decrease in capillary flow after CSD induction in adult mice [25]. This indicates that CSD induces a transient increase in local perfusion followed by a prolonged oligemia. We did not find post-CSD oligemia with LDF, but a sustained decrease in RBC velocity may indicate the presence of local oligemia after the passage of CSD in this experiment. A decrease and transient cessation of capillary flow were observed in neonatal rats [7]. We have also demonstrated transient slowing, with occasional full stop, of RBC flow in a single capillary in adult rats [30,32]. In the present experiment, decrease in RBC velocity was found during CSD (Intra-CSD) in some capillaries, and the velocity in a subset of such capillaries remained low even after passage of CSD (Inter-CSD). This indicates that the suppressive effect on RBC velocity is persistent, at least in some capillaries. In several capillaries, moving RBCs were not detected during CSD (Intra-CSD), but appeared after passage of the CSD wave (Inter-CSD). RBC flow stop may occur in such capillaries during CSD. As described in our previous report [32], it took several minutes for slowed-down RBC flow to return to the baseline level. As the DC potential deflection returned to the baseline level within one minute, slowed-down RBC flow can still be seen after the CSD wave has passed.

We observed not only slowed RBCs but also accelerated RBCs during CSD. Furthermore, we found some RBCs with extremely high velocities during CSD, and the capillaries in which these RBCs ran were straight. We have previously reported RBCs running at ultra-high velocity in single capillaries (up to 9.4 mm/sec); these RBCs might be missed with a conventional low-speed camera (30 fps), and the vessels may be thoroughfare channels or non-nutritional capillaries [33]. Our present results are consistent with the idea that the highly accelerated RBCs flow in thoroughfare channels and contribute at least in part to the elevation of CBF.

The increased CBF measured with LDF and the slowed-down RBC flow during CSD seem to be paradoxical. A similar phenomenon, that is, decreased RBC flow in some capillaries, was observed when regional CBF was greatly increased by topical application of nitroprusside (a nitric oxide donor) on the brain surface [28]. Inhomogeneous vasoreactivity to CSD was established by the observation that in smaller pial arteries, the initial vasoconstriction was limited and the subsequent vasodilation was more marked during CSD, whereas a much larger vasoconstriction and

smaller vasodilation were found in intracortical arterioles [7]. LDF provides the average blood flow of such inhomogeneous vessels to a depth of approximately 1 mm, and the value obtained is the product of RBC velocity and RBC flux. The observation area and the focus range in our experiment were limited to approximately 50 μm in thickness at the depth of layer I, and we focused on capillary flow, without arterioles or venules. Thus, possible reasons for the paradox may be as follows: vasoreactivity may vary with depth or with the types of vessels; the change in blood flow in the limited layer observed in our experiment may be different from the value indicated by LDF; or RBCs may pass through non-flowing or sparsely flowing capillaries during CSD (RBC recruitment), resulting in an increase in net flux of RBCs.

Neuro-Capillary Coupling

Heterogeneity of the changes in RBC velocity in capillaries and of the location of such capillaries was observed in our experiments. This means that RBC flow in capillaries within a small region is not uniformly controlled by the upstream arteriole. Rather, the capillary RBC flow seems to be actively controlled in response to neuronal requirements. A close correlation between topographical microflow and light transparency changes after topical application of potassium indicated that local depolarization of the neurons induces an immediate decrease, rapidly followed by an increase in microflow [29]. Transient constriction of parenchymal arterioles, often forming spindle-shaped strings, was reported in the early phase of CSD, followed by marked dilation [17]. CSD induced neuronal swelling in anesthetized mice [25] and in cortical slices of rodents [39], but both studies found that the cell volume of astrocytes did not change. However, we observed a morphological change in astrocytes during CSD [32]. Furthermore, a significant role of pericytes in neurovascular function was recently demonstrated [4]. Pericyte contraction induced by oxidative–nitrative stress caused capillary constriction and reduced RBC flow in mouse brain slices [37]. In addition to these facts, the results of our experiments provide further support for the hypothesis that the depolarized neurons alter adjacent capillary resistance through some physical and/or hemorheological mechanism, such as local cellular changes, that is, the phenomenon of so-called neuro-capillary coupling might be involved [32].

CONCLUSIONS

Administration of KCl onto the surface of the cerebral cortex induces repetitive CSD episodes, which involve DC potential deflection and propagate in the distal direction. Enhanced metabolism induces a PO_2 decrease (local hypoxia) and CBF increase to meet the enhanced requirement of O_2. Decrease in RBC velocity may enhance O_2 exchange efficiency to meet the increased O_2 demand, while RBC flow in some capillaries may be greatly enhanced, thereby contributing to the CBF elevation during CSD.

PERSPECTIVE

Potassium application elicited CSD accompanied with transient neuronal excitation and increase in CBF and metabolism in rats. We observed heterogeneous modulation of RBC velocity, including sustained decrease and remarkable increase. Whereas accelerated RBCs may be associated with CBF elevation, slowed-down RBCs may suggest the presence of a regional regulatory mechanism of capillary flow in brain.

ACKNOWLEDGMENTS

This work was supported by Grants-in-Aid for Scientific Research No. 22390182 (Suzuki, N) and No. 21591119 (Tomita, Y) from the Ministry of Education, Culture, Sports, Science, and Technology of Japan. This work was also supported by Otsuka Pharmaceutical Co., Ltd.

REFERENCES

1. Akcali D, Sayin A, Sara Y, Bolay H. Does single cortical spreading depression elicit pain behaviour in freely moving rats? *Cephalalgia* 30: 1195–1206, 2010.
2. Ayata C, Shin HK, Salomone S, Ozdemir-Gursoy Y, Boas DA, Dunn AK, Moskowitz MA. Pronounced hypoperfusion during spreading depression in mouse cortex. *J Cereb Blood Flow Metab* 24: 1172–1182, 2004.
3. Back T, Kohno K, Hossmann KA. Cortical negative DC deflections following middle cerebral artery occlusion and KCl-induced spreading depression: effect on blood flow, tissue oxygenation, and electroencephalogram. *J Cereb Blood Flow Metab* 14: 12–19, 1994.
4. Bell RD, Winkler EA, Sagare AP, Singh I, LaRue B, Deane R, Zlokovic BV. Pericytes control key neurovascular functions and neuronal phenotype in the adult brain and during brain aging. *Neuron* 68: 409–427, 2010.
5. Busija DW, Bari F, Domoki F, Horiguchi T, Shimizu K. Mechanisms involved in the cerebrovascular dilator effects of cortical spreading depression. *Prog Neurobiol* 86: 379–395, 2008.
6. Charles A, Brennan K. Cortical spreading depression-new insights and persistent questions. *Cephalalgia* 29: 1115–1124, 2009.
7. Chuquet J, Hollender L, Nimchinsky EA. High-resolution in vivo imaging of the neurovascular unit during spreading depression. *J Neurosci* 27: 4036–4044, 2007.
8. Fabricius M, Akgoren N, Lauritzen M. Arginine-nitric oxide pathway and cerebrovascular regulation in cortical spreading depression. *Am J Physiol* 269: H23–H29, 1995.
9. Hutchinson EB, Stefanovic B, Koretsky AP, Silva AC. Spatial flow-volume dissociation

of the cerebral microcirculatory response to mild hypercapnia. *Neuroimage* 32: 520–530, 2006.
10. Kocher M. Metabolic and hemodynamic activation of postischemic rat brain by cortical spreading depression. *J Cereb Blood Flow Metab* 10: 564–571, 1990.
11. Lacombe P, Sercombe R, Correze JL, Springhetti V, Seylaz J. Spreading depression induces prolonged reduction of cortical blood flow reactivity in the rat. *Exp Neurol* 117: 278–286, 1992.
12. Lauritzen M. Pathophysiology of the migraine aura. The spreading depression theory. *Brain* 117(Pt. 1): 199–210, 1994.
13. Lauritzen M, Jorgensen MB, Diemer NH, Gjedde A, Hansen AJ. Persistent oligemia of rat cerebral cortex in the wake of spreading depression. *Ann Neurol* 12: 469–474, 1982.
14. Leão A. Spreading depression of activity in cerebral cortex. *J Neurophysiol* 7: 359–390, 1944.
15. Mayevsky A, Weiss HR. Cerebral blood flow and oxygen consumption in cortical spreading depression. *J Cereb Blood Flow Metab* 11: 829–836, 1991.
16. Nielsen AN, Fabricius M, Lauritzen M. Scanning laser-Doppler flowmetry of rat cerebral circulation during cortical spreading depression. *J Vasc Res* 37: 513–522, 2000.
17. Osada T, Tomita M, Suzuki N. Spindle-shaped constriction and propagated dilation of arterioles during cortical spreading depression. *Neuroreport* 17: 1365–1368, 2006.
18. Piilgaard H, Lauritzen M. Persistent increase in oxygen consumption and impaired neurovascular coupling after spreading depression in rat neocortex. *J Cereb Blood Flow Metab* 29: 1517–1527, 2009.
19. Schiszler I, Takeda H, Tomita M, Tomita Y, Osada T, Unekawa M, Tanahashi N, Suzuki N. Software (KEIO-IS2) for automatically tracking red blood cells (RBCs) with calculation of individual RBC velocities in single capillaries of rat brain. *J Cereb Blood Flow Metab* 25(Suppl.): S541, 2005.
20. Seylaz J, Charbonné R, Nanri K, Von Euw D, Borredon J, Kacem K, Méric P, Pinard E. Dynamic in vivo measurement of erythrocyte velocity and flow in capillaries and of microvessel diameter in the rat brain by confocal laser microscopy. *J Cereb Blood Flow Metab* 19: 863–870, 1999.
21. Shinohara M, Dollinger B, Brown G, Rapoport S, Sokoloff L. Cerebral glucose utilization: local changes during and after recovery from spreading cortical depression. *Science* 203: 188–190, 1979.
22. Sonn J, Mayevsky A. Effects of anesthesia on the responses to cortical spreading depression in the rat brain in vivo. *Neurol Res* 28: 206–219, 2006.
23. Sukhotinsky I, Dilekoz E, Moskowitz MA, Ayata C. Hypoxia and hypotension transform the blood flow response to cortical spreading depression from hyperemia into hypoperfusion in the rat. *J Cereb Blood Flow Metab* 28: 1369–1376, 2008.
24. Sukhotinsky I, Yaseen MA, Sakadzic S, Ruvinskaya S, Sims JR, Boas DA, Moskowitz MA, Ayata C. Perfusion pressure-dependent recovery of cortical spreading depression is independent of tissue oxygenation over a wide physiologic range. *J Cereb Blood Flow Metab* 30: 1168–1177, 2010.
25. Takano T, Tian GF, Peng W, Lou N, Lovatt D, Hansen AJ, Kasischke KA, Nedergaard M. Cortical spreading depression causes and coincides with tissue hypoxia. *Nat Neurosci* 10: 754–762, 2007.
26. Tomita M, Gotoh F. Local cerebral blood flow values as estimated with diffusible tracers: validity of assumptions in normal and ischemic tissue. *J Cereb Blood Flow Metab* 1: 403–411, 1981.
27. Tomita M, Osada T, Schiszler I, Tomita Y, Unekawa M, Toriumi H, Tanahashi N, Suzuki N. Automated method for tracking vast numbers of FITC-labeled RBCs in microvessels of rat brain in vivo using a high-speed confocal microscope system. *Microcirculation* 15: 163–174, 2008.
28. Tomita M, Osada T, Unekawa M, Tomita Y, Toriumi H, Suzuki N. Exogenous nitric oxide increases microflow but decreases RBC attendance in single capillaries in rat cerebral cortex. *Microvasc Rev Commun* 3: 11–16, 2009.
29. Tomita M, Schiszler I, Fukuuchi Y, Amano T, Tanahashi N, Kobari M, Takeda H, Tomita Y, Ohtomo M, Inoue K. A time-variable concentric wave-ring increase in light transparency and associated microflow changes during a potassium-induced spreading depression in the rat cerebral cortex. In: Brain Activation and CBF Control; Exerpta Medica International Congress Series 1235, edited by Tomita M, Kanno I, Hamel E. Amsterdam: Elsevier Science, 2002, p. 439–447.
30. Tomita M, Schiszler I, Tomita Y, Tanahashi N, Takeda H, Osada T, Suzuki N. Initial oligemia with capillary flow stop followed by hyperemia during K^+-induced cortical spreading depression in rats. *J Cereb Blood Flow Metab* 25: 742–747, 2005.
31. Tomita Y, Tomita M, Schiszler I, Amano T, Tanahashi N, Kobari M, Takeda H, Ohtomo M, Fukuuchi Y. Repetitive concentric wave-ring spread of oligemia/hyperemia in the sensorimotor cortex accompanying K^+-induced spreading depression in rats and cats. *Neurosci Lett* 322: 157–160, 2002.
32. Tomita M, Tomita Y, Unekawa M, Toriumi H, Suzuki N. Oscillating neuro-capillary coupling during cortical spreading depression as observed by tracking of FITC-labeled RBCs in single capillaries. *NeuroImage* 56: 1001–1010, 2011.
33. Unekawa M, Tomita M, Osada T, Tomita Y, Toriumi H, Tatarishvili J, Suzuki N. Frequency distribution function of red blood cell velocities in single capillaries of the rat cerebral cortex using intravital laser-scanning confocal microscopy with high-speed camera. *Asian Biomed* 2: 203–218, 2008.
34. Vinogradova LV, Koroleva VI, Bures J. Reentry waves of Leao's spreading depression between neocortex and caudate nucleus. *Brain Res* 538: 161–164, 1991.
35. Williams JL, Shea M, Jones SC. Evidence that heterogeneity of cerebral blood flow does not involve vascular recruitment. *Am J Physiol* 264: H1740–H1743, 1993.
36. Wolf T, Lindauer U, Obrig H, Dreier J, Back T, Villringer A, Dirnagl U. Systemic nitric oxide synthase inhibition does not affect brain oxygenation during cortical spreading depression in rats: a noninvasive near-infrared spectroscopy and laser-Doppler flowmetry study. *J Cereb Blood Flow Metab* 16: 1100–1107, 1996.
37. Yemisci M, Gursoy-Ozdemir Y, Vural A, Can A, Topalkara K, Dalkara T. Pericyte contraction induced by oxidative-nitrative stress impairs capillary reflow despite successful opening of an occluded cerebral artery. *Nat Med* 15: 1031–1037, 2009.
38. Zhang ZG, Chopp M, Maynard KI, Moskowitz MA. Cerebral blood flow changes during cortical spreading depression are not altered by inhibition of nitric oxide synthesis. *J Cereb Blood Flow Metab* 14: 939–943, 1994.
39. Zhou N, Gordon GR, Feighan D, MacVicar BA. Transient swelling, acidification, and mitochondrial depolarization occurs in neurons but not astrocytes during spreading depression. *Cereb Cortex* 20: 2614–2624, 2010.

J Acupunct Meridian Stud 2012;5(2):57—62

Available online at www.sciencedirect.com

Journal of Acupuncture and Meridian Studies

journal homepage: www.jams-kpi.com

RESEARCH ARTICLE

Effects of Trigger Point Acupuncture Treatment on Temporomandibular Disorders: A Preliminary Randomized Clinical Trial

Kazunori Itoh [1,*,†], Sayo Asai [1,†], Hideaki Ohyabu [2], Kenji Imai [1], Hiroshi Kitakoji [1]

[1] *Department of Clinical Acupuncture and Moxibustion, Meiji University of Integrative Medicine, Kyoto, Japan*
[2] *Department of Dentistry, Meiji University of Integrative Medicine, Kyoto, Japan*

Available online Feb 19, 2012

Received: Jun 20, 2011
Revised: Jan 5, 2012
Accepted: Jan 11, 2012

KEYWORDS
acupuncture;
chronic pain;
myofascial pain;
temporomandibular disorder;
TMD;
trigger point

Abstract
We compared the effects of trigger point acupuncture with that of sham acupuncture treatments on pain and oral function in patients with temporomandibular disorders (TMDs). This 10-week study included 16 volunteers from an acupuncture school with complaints of chronic temporomandibular joint myofascial pain for at least 6 months. The participants were randomized to one of two groups, each receiving five acupuncture treatment sessions. The trigger point acupuncture group received treatment at trigger points for the same muscle, while the other acupuncture group received sham treatment on the trigger points. Outcome measures were pain intensity (visual analogue scale) and oral function (maximal mouth opening). After treatment, pain intensity was less in the trigger point acupuncture group than in the sham treatment group, but oral function remained unchanged in both groups. Pain intensity decreased significantly between pretreatment and 5 weeks after trigger point ($p < 0.001$) and sham acupunctures ($p < 0.050$). Group comparison using the area under the curve demonstrated a significant difference between groups ($p = 0.0152$). Compared with sham acupuncture therapy, trigger point acupuncture therapy may be more effective for chronic temporomandibular joint myofascial pain.

* Corresponding author. Department of Clinical Acupuncture and Moxibustion, Meiji University of Integrative Medicine, Kyoto 629-0392, Japan.
E-mail: k_itoh@meiji-u.ac.jp
† These authors contributed equally to this study.

doi:10.1016/j.jams.2012.01.013

1. Introduction

Myofascial pain is the most common temporomandibular disorder (TMD) [1]. This condition has also been called facial arthromyalgia, temporomandibular joint (TMJ) dysfunction syndrome, myofascial pain dysfunction syndrome, craniomandibular dysfunction, pain dysfunction syndrome, and myofascial pain dysfunction. The etiology of myofascial pain is multifactorial [2]. Consequently, many different therapies—some conservative, reversible, or irreversible—have been advocated for patients with myofascial pain. A number of successful treatments have been reported such as physiotherapy [3] and pharmacologic interventions [4].

TMD is basically treated using conservative approaches such as occlusal splints, occlusal adjustment, jaw exercise, and counselling, but other options have been used with good clinical results [5–7]. Acupuncture has been reported to have a beneficial role in the management of TMD [5,8–10]. Five randomized controlled trials found that the beneficial effects of acupuncture were similar to those of stabilization splint therapy in the management of TMD [11]. However, a systematic review found no trials with controls for the possible placebo effects of acupuncture, although studies suggest that acupuncture is effective in the treatment TMJ pain and dysfunction [11]. Therefore, due to lack of adequate controls for the placebo effect of acupuncture, the true efficacy of acupuncture has yet to be ascertained.

Our main aim in this study was to determine whether acupuncture at trigger points (compared with sham acupuncture treatment) is an effective treatment for chronic TMJ myofascial pain.

2. Methods

2.1. Patients

Students of an acupuncture school in Kyoto, Japan (Meiji University of Integrative Medicine), who had been clinically diagnosed as having TMD were recruited. Inclusion criteria were (a) orofacial pain lasting for 6 months or longer, (b) a Helkimo clinical dysfunction index of I or III, (c) no acupuncture in the previous 6 months, and (d) failure to respond to the medications prescribed by a specialist. Exclusion criteria were (a) major trauma or systemic disease, and (b) other conflicting or concurrent treatments. A total of 16 patients (five women, 11 men aged 19–24 years) who gave written informed consent were enrolled and randomly allocated to a trigger point acupuncture (TrP) group or sham (SH) group by use of a computerized randomization program. Ethical approval for this protocol was given by the ethics committee of Meiji University of Integrative Medicine.

2.2. Design

This clinical trial was a single-blinded, randomised, sham-controlled trial that used block randomisation to allocate patients to receive one of the two different acupuncture treatments. Each patient received a total of five treatments, one per week, each lasting 30 minutes, and follow-up measurements were taken at 10 weeks after the first treatment.

2.3. Blinding

Patients were blinded to their treatment assignment. They were told before randomization that they would be allocated to one of two groups. The measurements were performed by an independent investigator who was not informed about the treatment sequence or the treatment the patient received before each measurement. Prior to treatment, the patients covered their eyes with an eye mask to ensure that they did not know which treatment they were receiving.

2.4. Treatment

2.4.1. TrP group

The TrP group received treatment at myofascial trigger points. The correct application of the technique requires experience in palpation and localization of taut muscle bands and myofascial trigger points. Precise needling of active myofascial trigger points provokes a brief contraction of muscle fibers. This local twitch response should be elicited for successful therapy, but it may be painful and post-treatment soreness is frequent [1,12]. In this study, the most important masticatory and cervical muscles were examined for myofascial trigger points (Table 1).

Disposable stainless steel needles (0.2 mm × 50 mm, Shizuoka-shi, Shizuoka, Japan, Seirin) were inserted into the skin over the trigger point to a depth of 5–15 mm, appropriate to the muscle targeted, and the 'sparrow pecking' technique was used to elicit a local muscle twitch response. After the local twitch response was elicited or a reasonable attempt made, the needle was retained for a further 15 minutes. The mean number of insertions was 4.2.

2.4.2. SH group

The SH group also received treatment at myofascial trigger points. The methods of choosing trigger points were the same. Similar stainless steel needles (0.2 mm × 50 mm, Shizuoka-shi, Shizuoka, Japan, Seirin) were used, but the tips were cut off to prevent the needle from penetrating the skin. The cut ends were manually smoothed with sand paper under clean conditions [13]. The acupuncturist

Table 1 Muscles treated in the two trigger point acupuncture groups.

Muscle	Trigger point group	Sham group
Temporalis	4	5
Masseter	7	8
Lateral pterygoid	7	8
Digastricus	2	2
Sternocleidomastoideus	4	4
Trapezius	5	4
Splenius capitis	1	3
Other	1	4